



2021 8th International Conference on Power and Energy Systems Engineering (CPESE 2021),  
10–12 September 2021, Fukuoka, Japan

# Parametric sensitivity analysis of rotor angle stability indicators: Simulation case

Ashish Shrestha\*, Francisco Gonzalez-Longatt

*Department of Electrical Engineering, Information Technology and Cybernetics, University of South-Eastern Norway, Porsgrunn, Norway*

Received 10 November 2021; accepted 16 November 2021

Available online xxxx

## Abstract

Because power electronic converter (PEC) dominated power generators do not provide the rotational inertia and the proportion of synchronous generators is reducing, the modern electrical grids are confronting a challenge of transient stability as the penetration rate rises. Analyzing the system characteristics is important for minimizing possible instabilities during regular operation as well as during emergencies. In this article, the parametric sensitivity of indicators for rotor angle stability is analyzed by taking a case study of a power system. The indicators are identified and investigated for different case scenarios with varying inertia constants. From the study, it is observed that if the inertia in any segment of a power system is lowered, the critical fault clearing time (CCTs) for an individual element will be decreased. Although all cases and sub-cases used in the analysis were found to be stable, the reducing inertia constant has a substantial influence on the results.

© 2021 The Author(s). Published by Elsevier Ltd. This is an open access article under the CC BY license

(<http://creativecommons.org/licenses/by/4.0/>).

Peer-review under responsibility of the scientific committee of the 2021 8th International Conference on Power and Energy Systems Engineering, CPESE 2021.

*Keywords:* Power system dynamics; Power system stability; Low inertial power system

## 1. Introduction

The huge integration of Distributed Generation Resources (DGR) and the quickly increasing PEC-based technologies has forced power networks to turn out to be complicated than in the past. All levels of the power system are undergoing significant transformations, including utilization, distribution, transmission, and generation. The current power system is undergoing substantial changes as a result of this rapid development; one of the key reasons for this is the reduction of system inertia as a result of these PEC-based technologies [1,2]. The majority of power generators in a traditional power system were synchronous; considered as a source of system's inertia in a power grid, however, the percentage of synchronous generators is decreasing now these days [3]. Furthermore, PEC-based technologies used in utilization, distribution, transmission, and generation level do not contribute to system inertia, which decreases system inertia in the power grid, resulting in extreme variations in system's dynamics [4].

\* Corresponding author.

*E-mail addresses:* [Ashish.Shrestha@usn.no](mailto:Ashish.Shrestha@usn.no) (A. Shrestha), [fglongatt@fglongatt.org](mailto:fglongatt@fglongatt.org) (F. Gonzalez-Longatt).

<https://doi.org/10.1016/j.egy.2021.11.233>

2352-4847/© 2021 The Author(s). Published by Elsevier Ltd. This is an open access article under the CC BY license (<http://creativecommons.org/licenses/by/4.0/>).

Peer-review under responsibility of the scientific committee of the 2021 8th International Conference on Power and Energy Systems Engineering, CPESE 2021.

Not only that, but the fraction of the penetration, fault location, and severity all affect the DGR-integrated power system's transient stability [5]. Titlens et al. discussed the importance of inertia in the operation and control of a power system, demonstrating that decreasing system inertia leads to a high Rate of Change of Frequency (RoCoF) and frequency variation, potentially increasing system instability [6]. The DGRs are installed at a low voltage level in the distribution system, which raises the quantity of fault current. As a result, widespread use of DGRs may cause issues with overall transient stability, frequency response, fault ridding capability, load-following capability, voltage responsiveness, and system regulation [7].

Impact assessment is a critical activity in the planning and operation of a system since an unknown proportion of factors can cause system instability and even blackout, particularly after a malfunction. Some experiments were carried out to evaluate the system performance and sensitivity in different modes of operation. Tamimi et al. studied the influence of solar PV penetration levels using small-signal stability for real data from the Ontario power system and its neighbors, concluding that distributed solar systems are more favorable than single solar farms in terms of power system stability [8]. The eigenvalue analysis, on the other hand, revealed that DGR penetration has no effect on small-signal stability [8]. On next side, Pieter Tielens determined that as the inertia decreases, the eigenvalues migrate toward the negative axes of real part with weak damping, and the system's stability becomes vulnerable to the location of the generation plant [9]. The CCTs for a micro grid under fault situations were studied by Wang et al. who discovered that the penetration level and the turbine's crowbar protection insertion time are extremely sensitive to the CCTs [10]. Sadhana et al. used Lyapunov's stability criteria to conduct a small signal stability study for the grid-tied-DGR with the influence of uncertain penetration of wind turbines, and found that the penetration has no effect on the low-frequency oscillation [11].

Different results and conclusions are presented in research for a variety of case studies, which may mislead the audience. The same factors have been discovered to be sensitive in some cases but not in others. However, parametric sensitivity analysis is critical for analyzing power system dynamics and reducing potential effects on a particular case system. In this article, the authors hope to give a parametric sensitivity analysis for the indicators of rotor angle stability with system inertia, which will aid in the analysis of the system's dynamics in both normal and contingency situations.

## 2. Method and assumptions

The CCT is the time during which the fault must be cleared in order for the system to remain stable, and it is critical to examine the performance evaluation, which is influenced by several factors such as the machine's inertia constant, critical clearing angle, system frequency, and initial power angle. CCT is critical for a power grid since the grid must return to its previous state within a certain amount of time. If the grid is unable to maintain its initial condition within that amount of time, a lower CCT causes system instability. Similarly, in the rotor angle stability study, the eigenvalue is the next indicator.

In a linear invariant system, the eigenvalues are the modes of the system that deliver the status of the system. For a stable grid system, all the modes must be stable; all conjugated eigenvalues ( $\alpha \pm j\omega$ ) must have the negative valued real portion. The fluctuations of electromechanical equipment must also be damped out as quickly as feasible for a stable grid system. The eigenvalue analysis results are reported in terms of damped frequency and damping factor for each mode for clarity. The system is considered classic during the study, hence there are  $2 * N$  modes for  $N$  generators. The generated modes should be subjected to a small-signal stability study.

The study of uncertainty, or how a parameter inside a purpose differs from differences in other variables, is known as parametric sensitivity analysis. It plays a significant role in assessing system performance from a planning perspective. The primary goal of this research is to offer a parametric sensitivity analysis of the indicators of rotor angle stability with system inertia (i.e., CCT,  $\lambda$ ,  $\omega$  and  $\zeta$ ). However, from a mathematical standpoint, the rotor angle stability analysis is very dimensioned and non-linear, and is provided by a set of differential–algebraic equations as shown in Eq. (1) [9]:

$$\frac{dX}{dt} = F(X, Y, P) \quad (1)$$

For the electromechanical dynamics,  $F$  is the function,  $X$  ( $X \in \mathbb{R}^{n_x}$ ) is the vector state variables,  $Y$  ( $Y \in \mathbb{R}^{n_y}$ ) is the vector of algebraic variables, and  $P$  ( $P \in \mathbb{R}^{n_p}$ ) is the vector of parameters. The dynamics of the power system

network, static loads, and the generator's stator equation are presented in Eq. (1). The following differential equation can be used to describe the dynamics of a synchronous machine:

$$\frac{2H}{\omega_s} \frac{\partial^2 \delta}{\partial t^2} = \frac{P_m - P_e}{S_{rated}} \quad (2)$$

Here in (2),  $H$  represents the inertia constant in MJ/MVA,  $S_{rated}$  represents the machine's rating in MVA,  $P_m$  and  $P_e$  represent mechanical and electrical power in MW, and  $\omega_s$  represents the angular frequency. For a multi-machine system, the simplified swing equation is as follows:

$$\frac{2H_{sys}}{\omega_s} \frac{\partial^2 \delta_{sys}}{\partial t^2} = P_m - P_e \text{ [in pu]} \quad (3)$$

When a multi-machine power system is studied, the dynamic behavior of an analogous system can be described as Eq. (4), where  $K_D$  is the damping constant for the equivalent system and  $\delta_0$  is the initial power angle.

$$\frac{2H_{sys}}{\omega_s} \frac{\partial^2 \delta_{sys}}{\partial t^2} + K_D \frac{\partial \delta_{sys}}{\partial t} + P_{max} \cos(\delta_0) \delta_{sys} = 0 \quad (4)$$

The mathematical equations for the CCTs, overall system frequency, and damping factor for a power system are given in Eqs. (5), (6), and (7). The indications are defined to be dependent on the system inertia using the Equations.

$$T_{CCT} = \sqrt{\frac{4H_{sys}}{\omega_s P_{max}}} (\delta_{CCT} - \delta_0) \text{ [in second]} \quad (5)$$

$$\omega_{sys} = \sqrt{\frac{\omega_s P_{max} \cos \delta_0}{2H_{sys}}} \text{ [in rad/s]} \quad (6)$$

$$\zeta = \frac{1}{2} K_D \sqrt{\frac{\omega_s}{2H_{sys} P_{max} \cos \delta_0}} \quad (7)$$

The parametric sensitivity analysis of such indicators has been undertaken in this article with respect to the inertia constants as indicated in Eq. (8), where  $X$  represents the rotor angle stability indicators and  $i$  represents the system states.

$$\frac{\partial X}{\partial H_i} = (i, i > 0) \quad (8)$$

From these mathematical expressions, it can be reasoned that the indicators are dependent on the inertia constant, and that stability analysis of such indicators can be conducted for a specific case, which aids in the analysis of system dynamics under various operating conditions.

As indicated in Fig. 1, this research employs the IEEE 39 Bus New England power system as a case study, which includes 10 generators, 39 buses, and 33 connecting lines. Based on their geographical structure, the complete system is divided into three components (West, North, and South), which are separated by blue lines in Fig. 1. For the aggregated power system having many machines (i.e., G1), the West area is considered a single generator, whereas the North area comprises three generators (G8, G9, and G10), and the South area contains six generators (G2, G3, G4, G5, G6 and G7). For the analysis, all of the components of the power system are modeled in DIgSILENT PowerFactory, and the DIgSILENT Programming Language (DPL) is utilized as the scripting language for the execution task. The components' information is taken from a study [12]. The CCT values are evaluated using the transient stability assessment, as well as the small-signal stability assessment for the eigenvalues, damping, and damped frequency.

Three scenarios and six sub-cases were explored in this study for the sensitivity analysis of the inertia constant. In the first scenario, the inertia levels in the West and South were assumed to be normal, while those in the North were assumed to be low, as indicated in Table 1. Similarly, in the second scenario, the inertia level of the South area is assumed to be low, however, in the third scenario, both areas (North and South) are assumed to have low inertia levels. The nominal values of the inertia constants are regarded as the original value acquired from the source [12], however, five steps (50%, 60%, 70%, 80%, and 90% of nominal inertia value) have been implemented and examined with six sub-cases for low inertia value (i.e. base case H, 0.9H, 0.8H, 0.7H, 0.6H and 0.5H). For these three scenarios and sub-cases, essential indications of power system stability such as CCTs, eigenvalue points, damping, and damped frequency have been discovered, and inferences have been derived from the observed data.

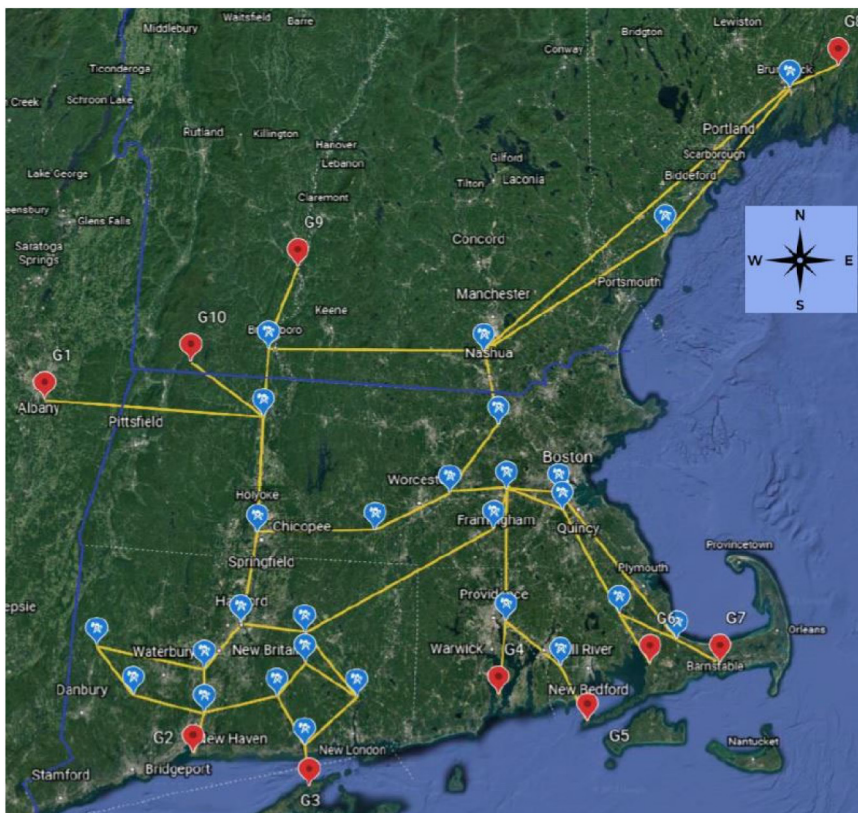


**Fig. 1.** IEEE 39 Bus New England power system with three zones division. The Generator buses are marked with red place-marks, PQ buses are marked with blue place-marks, and transmission lines are marked with yellow lines in the diagram. (For interpretation of the references to color in this figure legend, the reader is referred to the web version of this article.)

**Table 1.** Assumed cases for the sensitivity analysis.

Scenarios	West	North	South
a	Normal	Low	Normal
b	Normal	Normal	Low
c	Normal	Low	Low

### 3. Result and discussion

The CCTs at each transmission line have been identified for the case study of the 39 Bus New England power system by evaluating the three scenarios and six sub-cases. During the study, a defect is first induced in a transmission line, and the DPL is then utilized to determine the CCTs for each transmission line. In Fig. 2, the simulation results have been represented and presented. Fig. 2(a), (b), and (c) show the CCTs achieved for each transmission line for various inertia constant values (i.e.,  $H$ ,  $0.9H$ ,  $0.8H$ ,  $0.7H$ ,  $0.6H$ , and  $0.5H$ ), grouped for the three situations listed in Table 1. When demonstrated in Fig. 2, the CCTs of most transmission lines fall as the inertia constant decreases. Because the overall system inertia is decreased in the same way (i.e.,  $H_a > H_b > H_c$ ), scenario ‘b’ has a higher difference rate than scenario ‘a’, and scenario ‘c’ has a higher difference rate than the other two scenarios. The CCTs for transmission lines near the G1 (i.e., Line 03–04, Line 01–39, Line 09–39, and Line 01–02) are significantly higher than the rest in all circumstances. The CCTs in different sections of the power system have been detected in different scenarios with all sub-cases to investigate the rationale for this. The detailed information on the CCTs is listed in Table 2.

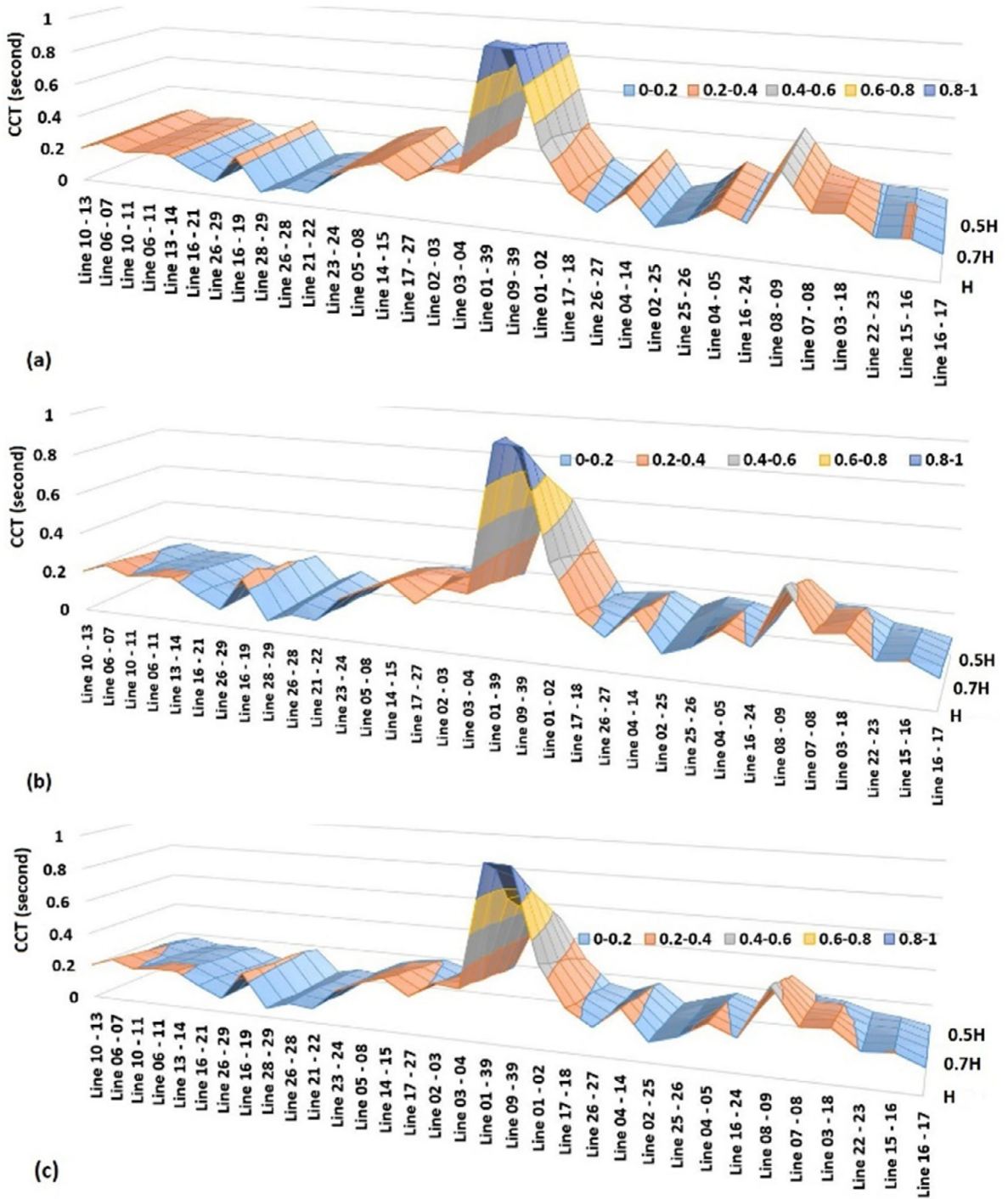


Fig. 2. Sensitivity analysis of the inertia constant in transmission lines with CCTs for three scenarios.

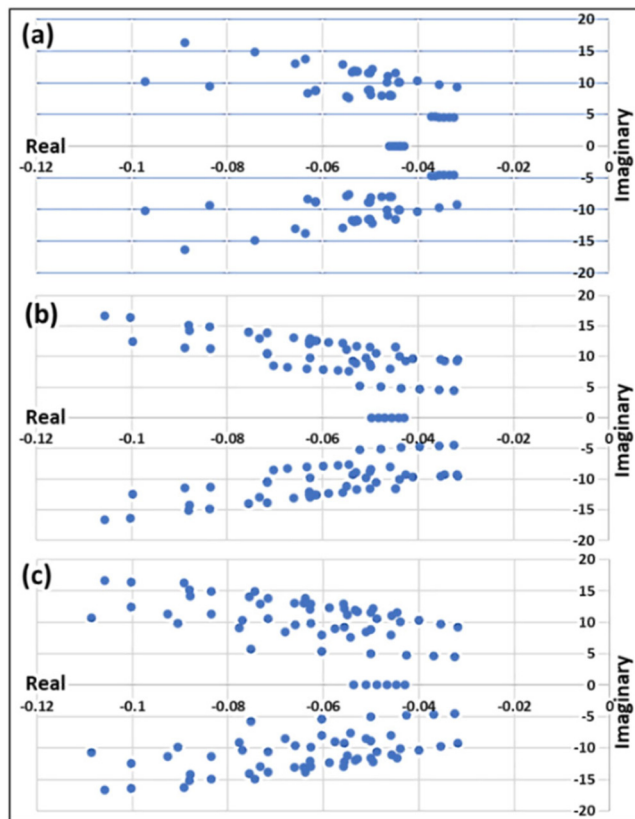


Fig. 3. Eigenvalue points for three scenarios.

Table 2. CCTs in various parts of the 33-bus New England system under various scenarios.

Scenarios		a	b	c
West	Base case	0.9960	0.9960	0.9960
	0.9H	0.9810	0.9505	0.9090
	0.8H	0.8790	0.8560	0.7575
	0.7H	0.8790	0.7195	0.6740
	0.6H	0.8785	0.6285	0.5905
	0.5H	0.8330	0.5680	0.4995
North	Base case	0.2033	0.2033	0.2033
	0.9H	0.1986	0.1996	0.1901
	0.8H	0.1911	0.1873	0.1741
	0.7H	0.1817	0.1778	0.1608
	0.6H	0.1693	0.1663	0.1446
	0.5H	0.1589	0.1531	0.1276
South	Base case	0.2415	0.2415	0.2415
	0.9H	0.2415	0.2265	0.2255
	0.8H	0.2415	0.2265	0.2083
	0.7H	0.2405	0.2093	0.1941
	0.6H	0.2405	0.1761	0.1701
	0.5H	0.2405	0.1580	0.1579

Table 2 clearly shows that as inertia diminishes at any one portion of the multi-machine power system, the CCTs of all components decrease, while the effect is more in the local area and less so in the neighboring area. Table 1 demonstrates that just the inertia of the North area is lowered in scenario ‘a’, while Table 2 shows that the decreased inertia affects the CCTs across the power system. Significant effects can be seen in scenario ‘c’, because the lowered inertia is higher in that scenario than in the others. It is evident from this that the CCTs are also affected by the location of the disturbance.

The small-signal stability analysis, on the other hand, is used to examine the case study’s stability as the system inertia constants decrease. The eigenvalue analysis is used to perform the small-signal stability study, and the results are given in Fig. 3. The information in Fig. 3(a), (b), and (c) depict the nature of real and imaginary eigenvalue point values for the three scenarios. All of the eigenvalue points are demonstrated to be on negative real parts, indicating that the system is stable in all scenarios. In comparison to the other two cases, the eigenvalue locus for scenario a may be clearly traced. The eigenvalue points disperse as the inertia constant decreases, as can be seen in the pictures.

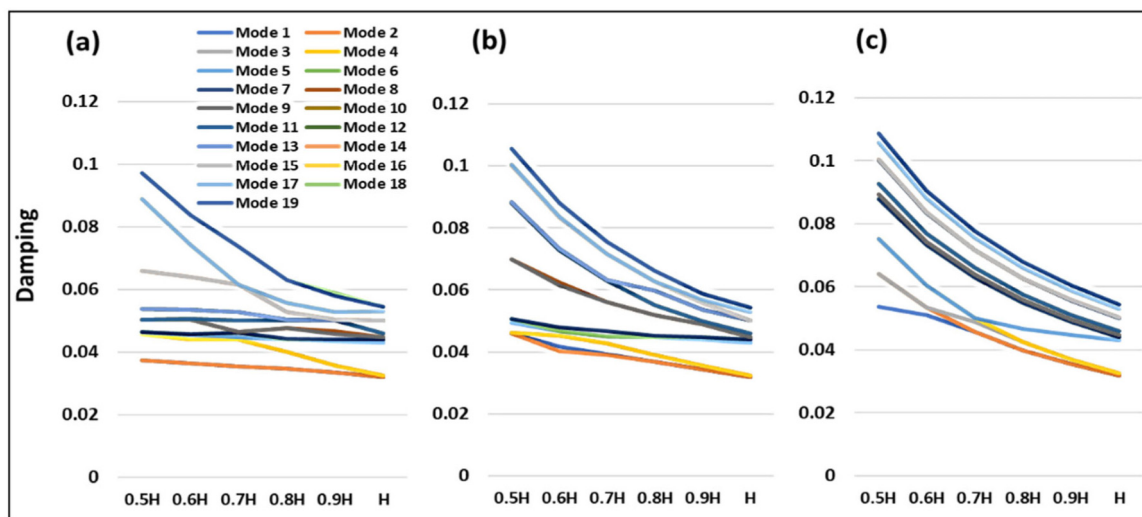


Fig. 4. Damping with the increasing order of inertia constant for three scenarios.

Fig. 4 depicts the sensitivity of the damping with respect to the inertia constant for the various scenarios. The results reveal that when the inertia constant increases, the damping reduces. In addition, the slope of the descent in scenario ‘b’ is higher than in scenario ‘a’, while scenario ‘c’ has a steeper drop than the rest. The peak value of damping for Mode 19 in the first scenario is 0.097143 at 0.5H inertia constant, and it reaches 0.05441 in the base case. The highest values for Mode 19 in the second and third situations, on the other hand, are 0.10565 and 0.108539. It is obvious from these numbers that the damping is quite sensitive to the inertia constant. Not only that, but the frequency is also affected by the inertia constant, as seen in Fig. 5. The damped frequency of Mode 17 in one case was 1.86792 Hz in the base case and 2.64161 Hz at the 0.5H inertia level, indicating a considerable change in the damped frequency with the change in the system’s inertia level.

#### 4. Conclusion

For the case study of the 39-bus New England power system, this paper gives a parametric sensitivity analysis of the rotor angle stability indicators. This analysis employs two types of power system analysis: transient and small-signal stability analysis. The research was performed to determine the values of indicators (i.e., CCTs, eigenvalue points, damping and damped frequency). After that, the indicators are evaluated, and the sensitivity of the inertia constants is determined for three different scenarios and six sub-cases. Because the third scenario has a considerable decline in system inertia, the results demonstrate that it has significant performance deviations when compared to the other two scenarios. Based on the simulation results, it is determined that the CCTs, damping, and frequency of a power system are very sensitive to system inertia. Also, the results suggest that if the inertia at a generator in

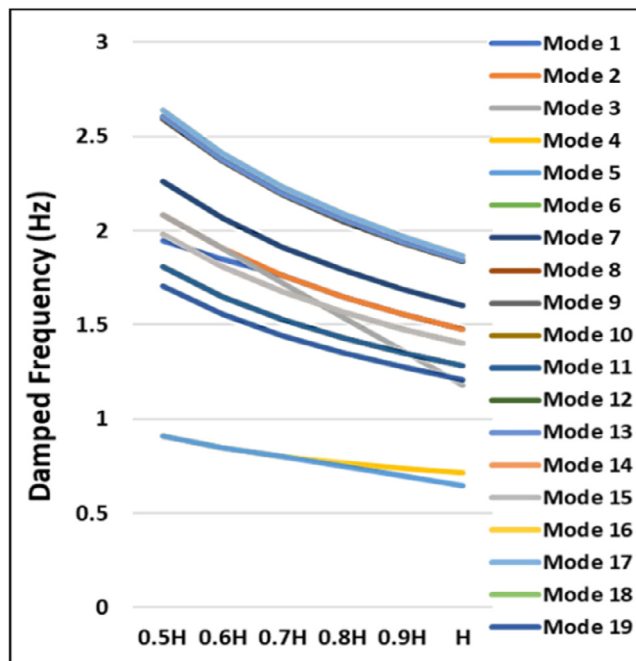


Fig. 5. The damped frequency with the increasing order of inertia constant.

a multi-machine power system is reduced, the CCTs for each component will be reduced, however, the impact will be greater in the local area and less in the surrounding area.

### Declaration of competing interest

The authors declare that they have no known competing financial interests or personal relationships that could have appeared to influence the work reported in this paper.

### Acknowledgments

Mr. Ashish Shrestha is thankful to the Department of Electrical Engineering, Information Technology and Cybernetics, University of South-Eastern Norway, Porsgrunn, Norway for the supports that he is receiving during his PhD. The extended version of this paper can be found as [13].

### References

- [1] A. Shrestha, B. Ghimire, F. Gonzalez-Longatt, A Bayesian model to forecast the time series kinetic energy data for a power system, *Energies* 14 (11) (2021) 3299.
- [2] A. Shrestha, F. Gonzalez-Longatt, Frequency stability issues and research opportunities in converter dominated power system, *Energies* 14 (14) (2021) 4184.
- [3] B. Kroposki, et al., Achieving a 100% renewable grid: Operating electric power systems with extremely high levels of variable renewable energy, *IEEE Power Energy Mag* 15 (2) (2017) 61–73.
- [4] T. Kerdphol, F.S. Rahman, Y. Mitani, Virtual inertia control application to enhance frequency stability of interconnected power systems with high renewable energy penetration, *Energies* 11 (4) (2018) 981.
- [5] N. Khadka, et al., Transient stability in renewable energy penetrated power systems: A review. In *RESSD 2020 international conference on role of energy for sustainable social development in 'new normal' era*, Nepal, 2020.
- [6] P. Tielens, D. Van Hertem, The relevance of inertia in power systems, *Renew Sustain Energy Rev* 55 (2016) 999–1009.
- [7] V. Vittal, et al., Impact of increased DFIG wind penetration on power systems and markets, PSERC Publication, 2009, p. 9.
- [8] B. Tamimi, C. Cañizares, K. Bhattacharya, System stability impact of large-scale and distributed solar photovoltaic generation: The case of Ontario, Canada, *IEEE Trans Sustain Energy* 4 (3) (2013) 680–688.



- [9] P. Tielens, Operation and control of power systems with low synchronous inertia, in: Faculty of engineering science, KU Leuven, Belgium, 2017.
- [10] Y. Wang, J. Ravishankar, T. Phung, A study on critical clearing time (CCT) of micro-grids under fault conditions, *Renew Energy* 95 (2016) 381–395.
- [11] S.G. Sadhana, S. Ashok, S. Kumaravel, Small signal stability analysis of grid connected renewable energy resources with the effect of uncertain wind power penetration, *Energy Procedia* 117 (2017) 769–776.
- [12] T. Athay, R. Podmore, S. Virmani, A practical method for the direct analysis of transient stability, *IEEE Trans Power Appar Syst* (2) (1979) 573–584.
- [13] A. Shrestha, F. Gonzalez-Longatt, Parametric sensitivity analysis of rotor angle stability indicators, *Energies* 14 (16) (2021) 5023.